Physics of Transition Metal Oxides

Lecture 8

Magnetic oxides

Magnetic insulators:

As the name implies, magnetic insulators have an energy gap and unpaired electrons, which give rise to the magnetic properties. $\chi_p = C/(T - \Theta)$

			Magnetic properties		
Compound	Band gap (eV)	$d-d$ transitions (eV)	S	Θ(K)	T_N(K)
Binaries					
Cr_2O_3	3.3	2.1,2.6	$\frac{3}{2}$	-550	308
MnO	3.6	2.2,2.9,3.5	$\frac{5}{2}$	-417	118
MnO_2	-	-	$\frac{3}{2}$	-1000	92
FeO	2.4	1.2	2	-500	198
αFe_2O_3	1.9	1.4,2.1,2.6,2.9	$\frac{5}{2}$	-3000	950
CoO	2.6	1.1,2.0,2.3	$\frac{3}{2}$	-300	292
NiO	3.8	1.1,1.8,3.2	1	-2000	523
CuO	1.4	?	$\frac{1}{2}$	-	226
Ternaries					
$LaVO_3$	-	-	1	-300	137
$LaCrO_3$	-	-	$\frac{3}{2}$	-600	300
$LaMnO_3$	-	-	2	-	100
$LaFeO_3$	-	-	$\frac{5}{2}$	-2000	750
$Y_3Fe_5O_{12}$	3	Many	$\frac{5}{2}$	-	559

Cox92 p.134

Notes regarding the table:

The band gap (optical) can only be measured in very pure stoichiometric materials. Any impurities, defects, or $d-d$ transitions would make the measurement inaccurate.

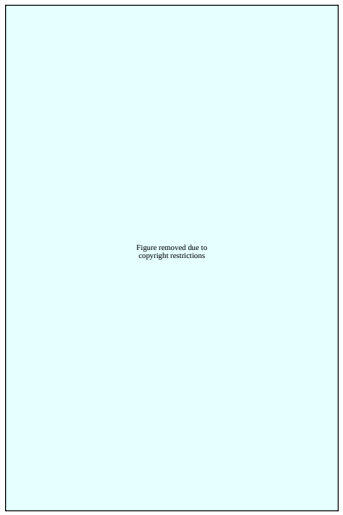

The gap can also be estimated from the activation energy for conductivity, but unfortunately, the defects provide most of the conductivity (not intrinsic carriers). Such measurements underestimate the gap width.
Direct measurements by x-ray absorption or emission are disturbed by core hole effects.
The most reliable data comes from photoelectron emission and inverse photoelectron spectroscopy. This example is for NiO, showing a gap of $\approx$ 4 eV. Optical absorption edge is at 3.8 eV. Photoelectron measurement of insulators is unfortunately difficult due to charging effects.

PRL 53 (1984) 2339

$d-d$ transitions

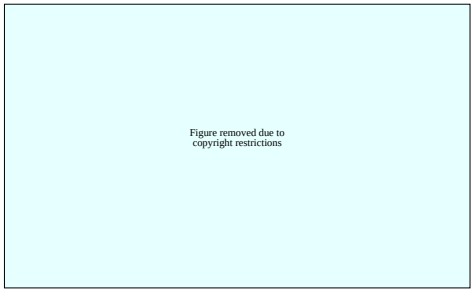

Surf. Sci. 152-153 (1985) 791

Even when defect-free samples are available, the $d-d$ transitions are unavoidable. These can be measured optically (the previous table) or by electron energy loss spectroscopy (EELS). Although EELS is a surface technique, the spectra apparently reflect the bulk properties, as shown in this spectrum for NiO. The optical $d-d$ transitions are at 1.1, 1.8, and 3.2 eV.

The magnetism above the ordering temperature follows a Curie-Weiss law

$$\chi_p = C/(T - \Theta),$$

where the Curie constant is

$$C = N\mu_0\mu_{\text{eff}}^2/(3k).$$

N is the number of magnetic ions and the effective magnetic moment is for many d^n ions

$$\mu_{\text{eff}} = 2[S(S+1)]^{1/2}\beta.$$

The ordering temperatures are usually around 100 K, indicating that the interaction energies are around 0.01 eV.

The band gap

Should we look at localized d^n ions or use band theory?

We have already discussed band descriptions of magnetic materials (Stoner enhancement, spin density waves).

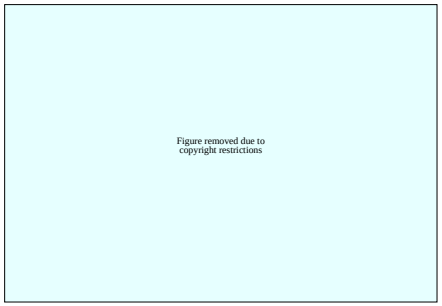

This shows the importance of different terms in the calculation of band gaps for MnO (right) and NiO (left) with a spin-dependent band model. The most important term is the exchange splitting, which gives the energy difference between spin-up and spin-down electrons on a given ion. Another important parameter is the band width (around 1 to 2 eV).

PRB 30 (1984) 4734

The difficulties here are:

- The estimated gap is too small, 0.5 eV instead of 3 to 4 eV.
- The experimental values for exchange splitting and crystal-field effects is around 1 eV. There appears to be no way of getting a 4 eV gap.
- The gap does not change much, or disappear at the ordering temperature. The calculated gap depends on spin interactions.
- The electronic configuration of MnO is $3d^5$, i.e. all levels are half-filled. In NiO, Ni is $3d^8$, i.e. the t_{2g} levels are full and e_g is half-full. This produces the gap. CoO has $3d^7$ and should thus be a metal. In fact, it has a similar gap as MnO and NiO.

Many of these problems are probably caused by the difficulty of including a correct ground-state description in the model.

Magnetic ordering:

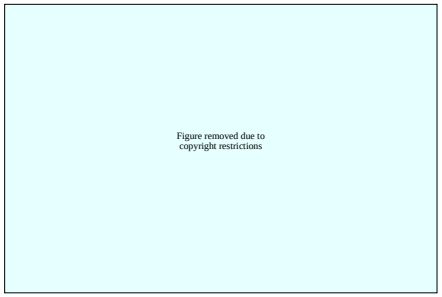

Most magnetic insulators are antiferromagnetic. Susceptibility drops below the *Néel temperature*. For example, in MnO $T_\mathrm{N} = 120$ K and below this temperature susceptibility is anisotropic. The reference direction is [111].

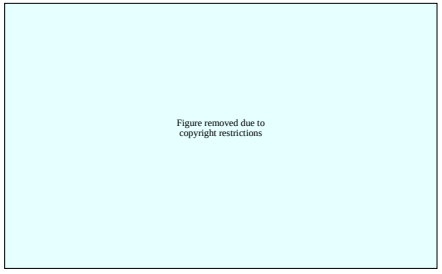

In case of antiferromagnetic order, a crystal has two *sub-lattices* of magnetic ions with different spin orientations. Magnetic order can be detected by neutron scattering because the spin of a neutron interacts with the spins in the crystal. The new peaks that appear below T_N would have indices like $(\frac{1}{2}, \frac{1}{2}, \frac{1}{2})$, indicating the presence of an enlarged magnetic unit cell.

Cox92 p.143

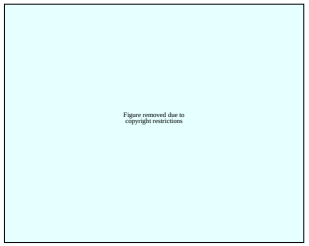

In most monoxides, like MnO, FeO, CoO, NiO, spins are in (111)-oriented sheets. Neighboring sheets have antiparallel spins. The actual spin direction deviates from the 111 direction slightly. This type of order is caused by next-nearest-neighbor interactions across an oxide ion (NaCl structure).

Cox92 p.145

In such oxides, the magnetic order also causes a slight lattice distortion, e.g. MnO becomes monoclinic belon T_N with an inclination of crystal axes of 0.62° (*magnetostriction*).

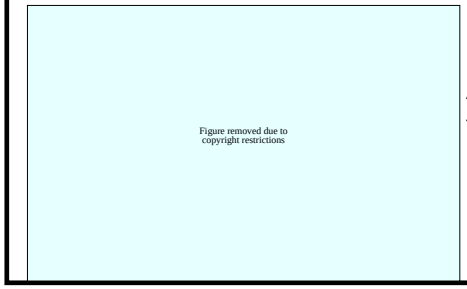

A variety of antiferromagnetic ordering geometries have been found by neutron diffraction studies. These structures, for example, have been identified in $La_{1-x}Ca_xMnO_3$.

Antiferromagnetic ordering via a bridging oxygen also goves G-type order in perovskites, for example, $LaVO_3$, $LaCRO_3$, $LaFeO_3$.

Some similar compounds have A-type ordering, such as $LaMnO_3$ where we have ferromagnetic order along the ab plane and antiferromagnetic order along the c direction.

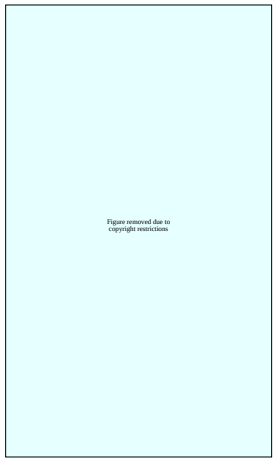

The magnetic unit cell of MnO_2 is much more compilacted, containing 7 structural unit cells. The spin directions form a spiral. This happens when several interactions compete: in MnO_2 the coupling between corner and body-centered ions, and between neighbors along the c-axis.

Cox92 p.145

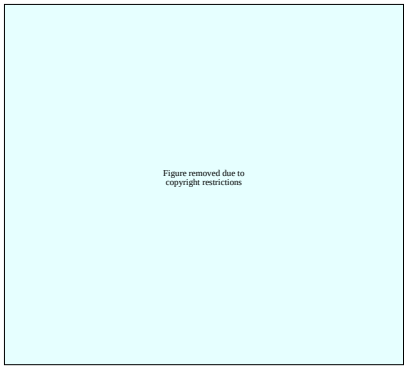

As the temperature is reduced below T_N, the magnetization of each sublattice saturates. Ideally the saturation value would be $2S\mu_B$. Typically a slightly lower value is seen, as this plot for Cr_2O_3 shows. Deviations are larger for small S and low-dimensional systems.

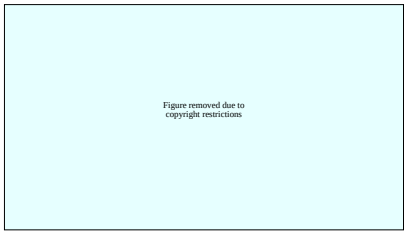

Inelastic neutron scattering can be used to measure also spin excitations, such as spin-waves or magnons. Spin waves would appear as an oscillation of the spin direction. These oscillations can propagate in a crystal with a characteristic momentum, much like a phonon.
the dispersion relation has been measured for MnO, as shown here. Characteristic energies are around 10 meV.

J. Phys. Chem. Solids 35 (1974) 433

Ferromagnetism is not common in insulators. a rather unusual example is $LiNiO_2$, which is ferromagnetic below 6 K. Weakly ferromagnetic systems appear when spins are canting. This can be seen in α-Fe_2O_3 between $T_N = 256$ K and 905 K.

a more common case is ferrimagnetism, where the sublattices have different spins that do not cancel, altthough they have antiferromagnetic alignment. This happens in YIG $Y_3Fe_5O_{12}$, where Fe is in different crystallographic sites. Each unit cell contains three tetrahedral sites and two octahedral sites, which do not cancel. In general this happens in *ferrites*.

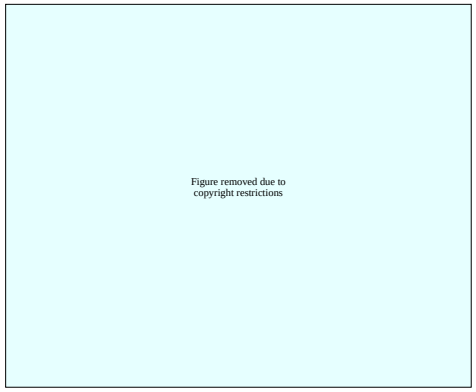

A large number of different magnetic phases can appear in a single family of compounds, depending on carrier concentration and temperature, as shown here for $La_{1-x}Ca_xMnO_3$. The phases include FI (ferromagnetic insulator) and canted antiferromagnetic spin regions (CAF).

Exchange interactions:

Direct magnetic coupling between metal ions in oxides is much too small to account for magnetic ordering that we have seen. Chemical bonding and the role of oxygen is often critical.

If we look at to weakly-interacting atoms, each with a single unpaired electron, the energy difference between singlet $S = 0$ and triplet $S = 1$ states is

$$\Delta E = 2K - 4St,$$

where

- $2K$ is the potential exchange term. It represents the electron repulsion in the two states. Pauli exclusion principle requires that the overall wavefunction has to be antisymmetric with respect to interchange of electrons. The same principle leads to the Hund rule in a single atom. The effect is ferromagnetic, although weak in oxides because neighboring metal ions are far from each other.

- $-4St$ is the *kinteic exchange* term. It includes the orbital overlap integral, S, and hopping integral, t. In band calculations t is the integral that gives a width to bands. This term depends on the type of chemical bonding and has an antiferromagnetic character. Electrons that share an orbital would have a lower energy if their spins are antiparallel.

A crystal can thus be either ferromagnetic or antiferromagnetic, depending on the relative importance of these two terms. For example, when the orbitals of neighboring metal ions are orthogonal, only the potential exchange term contributes, giving a ferromagnetic system. Large orbital overlap would stabilize antiferromagnetic order.

In oxides we don't really have metal-metal interactions. What we do have are metal-oxygen-metal interactions. Such indirect overlap is responsible for *superexchange*. The most common case that we look at is a linear chain of metal and oxygen atoms.

Superexchange

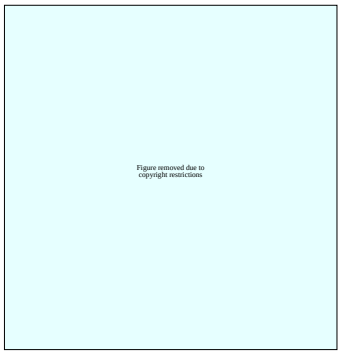

The ground state is antiferromagnetic (a). This ground state can mix with two types of charge transfer configurations (b) and (c). This is only possible for an antiferromagnetic configuration of metal spins.

Cox92 p.150

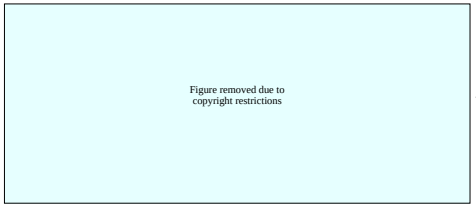

A very different result occurs if a ligand couples two metals at a 90° angle, as happens in halides. Each metal interacts with a different p-orbital of the ligand. Since the two p orbitals are orthogonal, the kinetic term is zero and the potential term dominates (ferromagnetic). Hund's rule shows why the ligand favors parallel spins in the two p orbitals.

The 90° configuration is unusual in oxides, although it can occur in rack-salt lattices with a composition AMO_2. The metals A and M should occupy neighboring layers. An example would be $LiCoO_2$, which appears to have a very narrow d band due to this configuration. $LiNiO_2$ is a rare ferromagnetic insulating oxide with this structure.

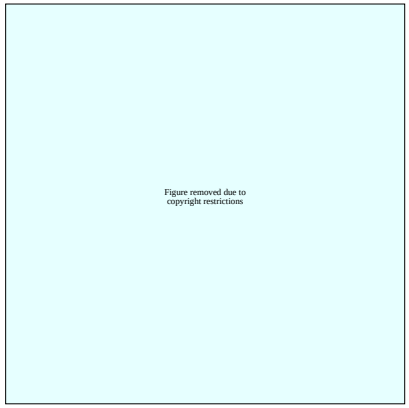

Cox92 p.152

In special cases, even a 180° M-O-M chain can give a ferromagnetic ground state. This happens when an occupied orbital couples with an empty orbital of a neighboring ion. An example is the ferromagnetic in-plane order of $LaMnO_3$. The d^4 Mn^{3+} ion has a strong co-operative Jahn-Teller distortion. Within the ab-plane, long and short M-O bonds alternate. the orientation of the single occupied e_g orbital is different at neighboring sites. an occupied orbital thus interacts with an empty orbital. An electron can thus transfer from one ion to next. Hund's coupling between different orbitals at a single site results in an overall ferromagnetic configuration.
Between planes, we have the normal antiferromagnetic interaction, giving an A-type antiferromagnet.

We have looked at the band model and seen that even in metallic oxides a simple band description does not fit experimental results very well. Different measurement techniques do not give consistent results either.

An important feature of oxides is the relatively small band width of d electrons close to the Fermi level. This leads to a high density of states and significant electron-electron interactions, or *correlations*. Such interactions also affect magnetic ordering in oxides.

This can be seen in e.g. $LaNiO_3$ or $LaCuO_3$, which show a strong Stoner enhancement or when $UN(E_F) \geq 1$, spontaneous ferromagnetic ordering (*band magnetism*). The magnetic susceptibility is much larger than expected based on $N(E_F)$.

Spontaneous order does not need to be ferromagnetic, it is equally possible to get an antiferromagnetic ordering with spin-density waves.

In general, we would expect to see an increase of ordering temperature with the decrease of band width, until metallic conductivity breaks down and we get a magnetic insulator.

Tiny changes in the structure of a material can have a large effect on magnetic ordering. $CaRuO_3$ and $SrRuO_3$ are very similar structurally, but $SrRuO_3$ is a ferromagnet with $T_C = 160$ K, but $CaRuO_3$ is non-magnetic.

CrO_2

CrO_2 is a well-known magnetic metallic oxide, widely used for magnetic recording. The crystal has the rutile structure. The Fermi level is within the t_{2g} part of the Cr $3d$ band. The d band has 2 electrons.

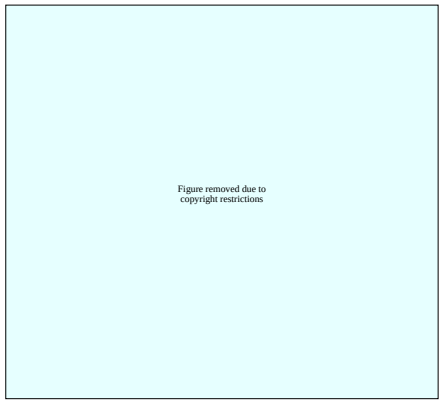

The splitting between the spin-up and spin-down electrons is comparable to the t_{2g} band width, giving a nearly 100% spin polarization. The measured saturation moment is around $2\mu_B$ per chromium. The Fermi level is within the gap of the minority spin electrons and CrO_2 is therefore known as a *half-metallic ferromagnet*. The Curie temperature is 177°C.

Example system: Ruthenates

Ruthenates form a series of Ruddlesden-Popper phases with a general formula of $Sr_{n+1}Ru_nO_{3n+1}$, with $n = 1, 2, 3$ and ∞. Depending on n, and possibly with Ca doping, the compounds can show metal-insulator transitions, giant magnetoresistance, superconductivity, ferromagnetism, antiferromagnetism, and spin or charge density waves.

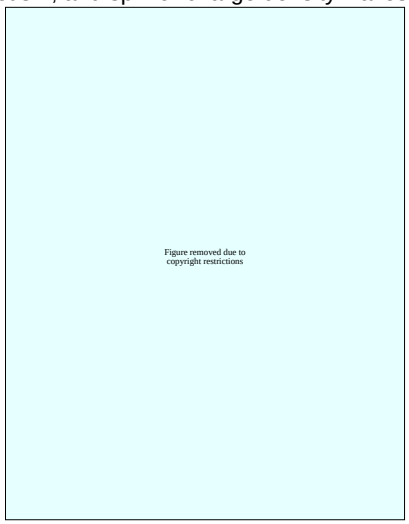

Mat. Sci. Eng. B63 (1999) 76

An important feature to note is that except for the $n = \infty$, the positions of the Ru ions alternate between the edge and the center of the unit cell. Therefore no oxygen ions within the intervening Sr-O or Ca-O layer are shared by the Ru ions of the adjacent layers. Accordingly, the number of Ru neighbors per ion decreases from six for $n = \infty$ to 16/3 for $n = 3$, to 5 for $n = 2$, and to four for $n = 1$. Due to this, exchange interactions and conductivity perpendicular to the RuO planes would be greatly affected by n. It is therefore important to look carefully which phase is actually present in a crystal.

Lattice parameters for $(Sr,Ca)_{n+1}Ru_nO_{3n+1}$ at T=295 K.

n	Comp	a(Å)	b(Å)	c(Å)	S.G	RuO_6 (rot/tilt)
1	Sr	3.87	3.87	12.74	I4/mmm	No
	Ca	5.41	5.49	11.96	Pbca	Yes
		3.83*	3.88*			
2	Sr	3.90	3.90	20.70	I4/mmm	No
	Ca	5.54	5.37	19.59	$Cmc2_1$	Yes
		3.91*	3.80*			
∞	Sr	5.53	5.57	7.85	Pbnm	No
		3.91*	3.93*			
	Ca	5.52	5.35	7.65	Pnma	Yes
		3.90*	3.78*			
	$SrTiO_3$	3.905				

* Perovskite pseudocell

Mat. Sci. Eng. B63 (1999) 76

Sr compounds show little RuO_6 tilt or rotation, but the Ca compounds are highly distorted due to the smaller ionic radius ($r_{Ca} = 1.0$ Å, $r_{Sr} = 1.18$ Å). Especially Ca_2RuO_4 has the RuO_6 octahedra rotated by 11.8° and tilted out of the RuO_2 plane by 12.7°. The lattice volume decreases by 1.3% when cooling a single crystal from 400 K to 90 K. In $SrRuO_3$, the oxygen octahedra are highly distorted with the edge lengths varying from 2.5 Å to 3.0 Å. The shape and orientation of the oxygen vibration ellipsoids is determined by the closest Ru neighbors, a result of the strong Ru4d-O2p hybridization.

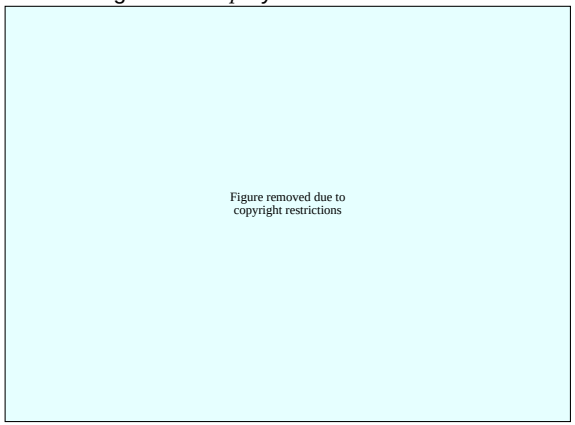

JMMM 206 (1999) 27

Oxygen stoichiometry:

Ru is normaly in the Ru^{4+} state in $SrRuO_3$, but can also be partly pushed to Ru^{5+} by oxygen loading. Oxygen loading also slightly distorts the structure:

Structure and resistivity of $Sr_2RuO_{4+\delta}$

a(Å)	c(Å)	δ	$\rho_{300K}(\Omega$cm)	$\rho_{150K}(\Omega$cm)	$\rho_{15K}(\Omega$cm)
3.876	12.732	0.0 (Ar anneal)	0.007	0.007	0.0072
3.870	12.739	0.2 (air anneal)	0.02	0.03	0.078
3.868	12.746	0.25 (O_2 anneal)	0.03	0.038	0.090

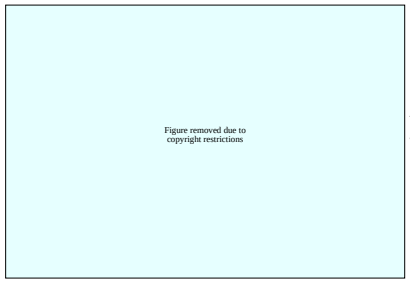

A TGA curve of oxygen loss from Sr_2RuO_4. The extra oxygen is supposed to enter interstitial sites in the rocksalt SrO layers, similar to La_2CoO_4, La_2NiO_4 or La_2CuO_4.

Mat. Chem. Phys. 56 (1998) 63

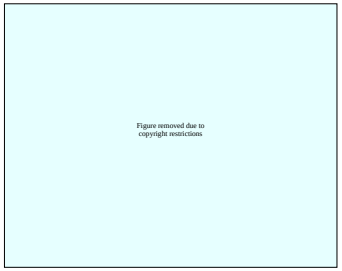

Loading of extra oxygen also causes a loss of conductivity.

Mat. Chem. Phys. 56 (1998) 63

The Ca_2RuO_4 is a more distorted structure and cannot be further oxidized or reduced. Ar or O_2 annealing breaks single crystals.

$Ca_3Ru_2O_7$ can be oxygen or argon annealed. Oxygen loading or depletion apparently affects the magnetic ordering more than the conductivity. Higher oxygen content gives higher conductivty, possibly due to hole-like carrier doping. Oxygen-poor material has lower conductivity and can become nonmetallic.

Thermogravimetry has shown that $Sr_3Ru_2O_7$ and $Ca_3Ru_2O_7$ start to lose oxygen at 1100°C and 1000°C, respectively. Oxygen annealing does not affect the Sr compound much.

Resistivity:

The Ca-compounds show a *metal-to-insulator transition* (MIT) at $T_{\rm MI} = 357$ K for $n = 1$ and 48 K for $n = 2$. The transition at 357 K is associated with a tetragonal to orthorombic structural transition.

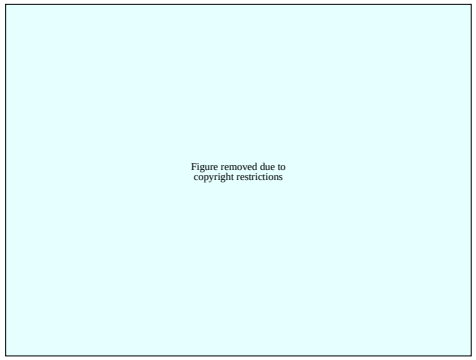

Mat. Sci. Eng. B63 (1999) 76

Below the transition ρ can be fitted with $\rho(T) = A\exp(T_0/T)^\nu$, with $\nu = 1/2$, characteristic of variable range hopping (VRH). The MIT temperature is much lower in the $n = 2$ compound and disappears completely in the $n = \infty$ phase. Although the $n = \infty$ phase is highly distorted, its resistivity is almost the same as that of $SrRuO_3$, showing that lattice distortions are not that important when the lattice has higher dimensionality.

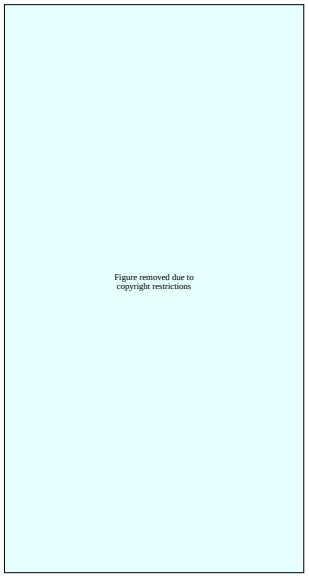

Mat. Sci. Eng. B63 (1999) 76

In a Mott-Hubbard model the MIT is controlled by the relative magnitude of the on-site Coulomb interaction U and the one-electron bandwidth W. A splitting between the lower and upper hubbard bands increases as U/W increases and for a half-filled band MIT occurs at $U/W \simeq 1$, where the Mott-Hubbard gap opens.
All Sr-compounds are metallic. The onset of ferromagnetism can be seen in the $n = 4$ and ∞ phases only. Conductivity at RT is still relatively bad, which is why these materials are categorized as ”bad metals”, i.e. the mean free path of of single-quasiparticle scattering is comparable to interatomic distances.

The MIT can presumably be controlled by gradual Ca/Sr substitutions. Sr_2RuO_4 is a good conductor and Ca_2RuO_4 is an insulator, probably because due to a large lattice distortion the electronic orbital overlap of d electrons, as in RNiO$_3$ is reduced. Reduced overlap also reduces W, the one-electron bandwidth. This increases the U/W ratio, resulting in an insulating structure. In $(Sr_{1-x}Ca_x)_{n+1}Ru_nO_{3n+1}$ compounds the W parameter can be tuned. For example, in $(Sr_{1-x}Ca_x)_3Ru_2O_7$, at $x \simeq 0.33$ the material first turns from a paramagnetic metal into an antiferromagnetic metal and then into an antiferromagnetic insulator.

In $SrRuO_3$ Ca substitution is not particularly sensitive. Substituting up to 65% of Ca ($Sr_{0.35}Ca_{0.65}Ru$ does not show significant change in resistivity, having $\rho_{300K} = 420\mu\Omega$cm.

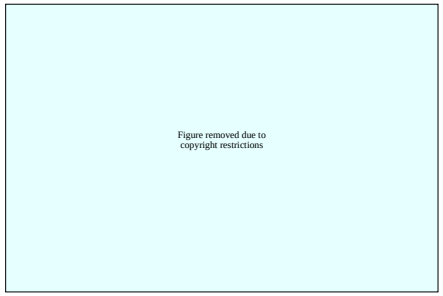

Resistivity becomes highly unisotropic in low-dimensional compounds like $Sr_3Ru_2O_7$. The kinks in resistivity are caused by rearrangements of the magnetic structure.

PRB 55 (1997) R672

Magnetic structure:

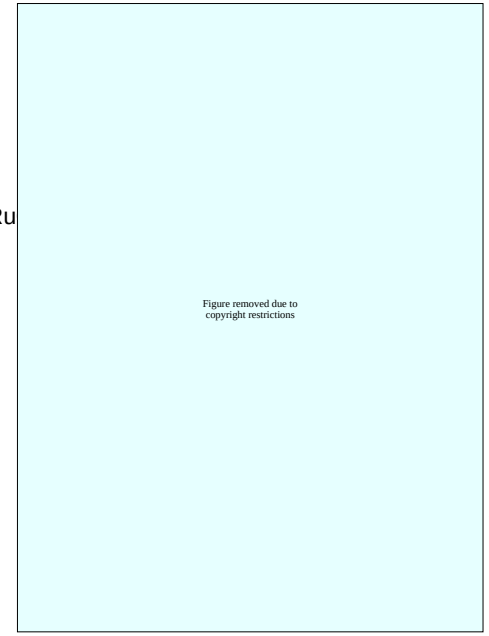

The origin of magnetism in ruthenates lies in the localized Ru4d shell. The crystal-field interaction splits the fivefold degenerate d-shell configuration into a ground-state t_{2g} triplet and an excited e_g doublet. The doublet is empty in Ru oxides. The $t_{2g} - e_g$ splitting is very large because of the large radial extent of the 4d shell. The t_{2g} orbitals are therefore filled first, giving a low-spin $S = 1$ configuration ($3d$ materials would probably choose the $S = 2$ configuration for nd^4).
In the diagram, γ is the low temperature electronic specific heat, μ_0 was measured at 5 K. All Sr-compounds except Sr_2RuO_4 have ferromagnetic ground states with T_c increasing with n.

Mat. Sci. Eng. B63 (1999) 76

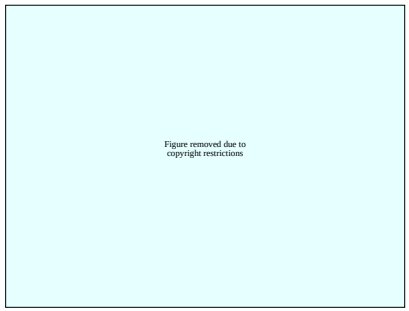

Antiferromagnetic behavior of Ca-compounds can be clearly seen in in susceptibility measurements. The Neel temperature drops with n (110 K for $n = 1$ and 56 K for $n = 2$).

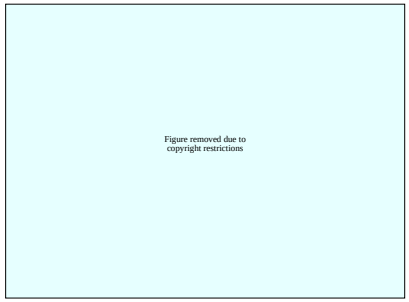

Replacing Ca with Sr causes the structure to become ferromagnetic and metallic (except for Sr_2RuO_4). The Curie temperatures are T_C=105 K, 148 K, and 165 K for $n = 2, 3$, and ∞, respectively. Sr_2RuO_4 is paramagnetic and becomes superconducting at 1.5 K (an unusual p-wave superconductor). The easy axis of magnetization lies in the ab plane for $n = 3$ and ∞, but along the c-axis for $n = 2$.

Mat. Sci. Eng. B63 (1999) 76

$SrRuO_3$

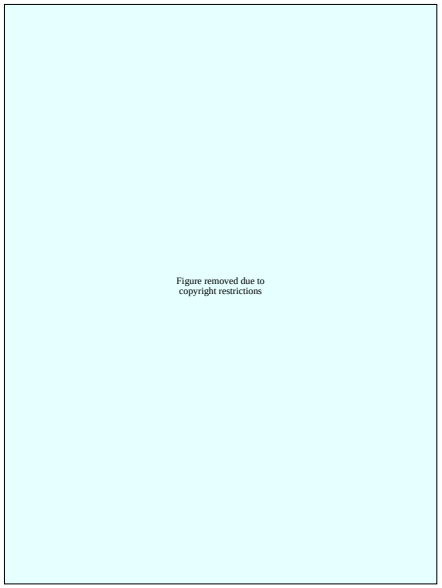

$SrRuO_3$ lattice parameters a, c, and V as a function of temperature. The fine lines represent the estimations of the phonon contribution to thermal expansion. Δa_m, Δc_m, and ΔV_m are the estimates of non-phononic contributions to the linear and volume thermal expansion. α_a, α_c, and α_V are the linear and volume thermal expansion coefficients. T_c=167 K.
Ferromagnetic ordering occurs at T_c=167 K. Above this temperature, thermal expansion can be fitted with a model which only considers the phononic contribution. At lower temperatures there is an anomaly caused by magnetic ordering. The nonphononic part along the a-direction $\Delta a_m/a$ id four times larger than along the c-direction $\Delta c_m/c$ at 100 K and the difference is even larger at lower temperatures.

JMMM 206 (1999) 27

Ca doping:

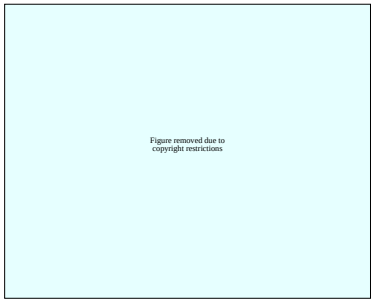

The magnetic behavior of $SrRuO_3$ can be tuned by partial substitution of Ca for Sr. The Curie temperature shifts lower as the doping level increases. Film thickness was 600 Å. Films were preapred by alternately depositing by PLD from $CaRuO_3$ and $SrRuO_3$, targets 1/4 of a unit cell per target at a time. Substrate was $LaAlO_3$.

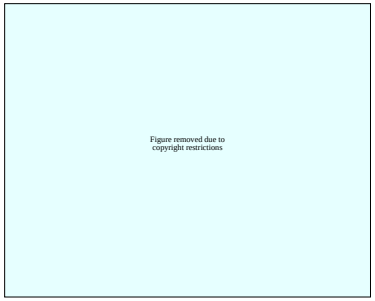

It was assumed that the magnetization at the Ru site can only be zero or have a fixed value, depending on the configuration of the dopants (Ca in the Sr site).

APL 70 (1997) 126

The probabilities of finding particular neighbor configurations is given by the binomial distribution

$$\frac{M(x)}{M(0)} = \sum_{n=0}^{n^*} \frac{p!}{(p-n)!n!} x^n (1-x)^{p-n}, \quad (1)$$

where n^* is a cut-off value, above which Ru sites do not affect each other ($n^* = 1$ for Ti doping and $n^* = 4$ for Ca doping, p and n are the maximum and actual numbers of near neighbor doping sites ($n \leq n^* \leq p$). For the Sr site $p = 8$ and for Ru site $p = 6$. The fit (dashed lines) shows that the binomial fit is good, which means that the dopants are randomly distributed. Sr can have up to 4 Ca neighbors and still maintain ferromagnetism at 5 K.

Sr_2RuO_4

Sr_2RuO_4 shows no local-moment magnetism or long-range magnetic ordering. It is, instead, a low-T_c superconductor with p-type pairing.

$Sr_3Ru_2O_7$

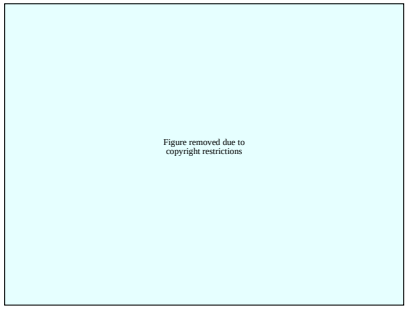

$(Sr,Ca)_3Ru_2O_7$ is probably the most interesting compound among the ruthenates in terms of magnetic properties. The two-dimensional nature of the lattice is also visible in the anisotropic magnetization behavior. The graphs show the main ferromagnetic ordering temperature 104 K and another spin-ordering transition at 66 K. The large difference in ZFC and FC magnetizations is typical of domain movement in ferromagnets.

PRB 55 (1997) R672

The anisotropy of $M(T)$ is very large below T_C and indicates that the easy axis of magnetization is along the (001) direction in $Sr_3Ru_2O_7$. (In $(Sr_{1-x}Ca_x)_3Ru_2O_7$ the easy axis gradually shifts to the [110] direction as x increases. In $Sr_{1-x}Ca_xRuO_3$ Ca-doping has the opposite effect, shifting the easy axis *out* of the ab plane).

The broad maximum in the $H \perp (001)$ dependence, however, resembles antiferromagnetic behavior. This can be understood if the spin arrangement is not collinear, i.e. ferromagnetically coupled along the c axis, but slightly canted due to antiferromagnetic coupling in the ab plane. The spin canting changes below 60 K. Spins can be realigned by applying an external magnetic field. In the c axis direction at 5 K the required field is 0.2 T. There is a sharp transition in $H \perp (001)$ $M(H)$ curves, indicating that a transition to perfectly aligned spins occurs in the 2-3 T range (higer fields at lower temperatures).

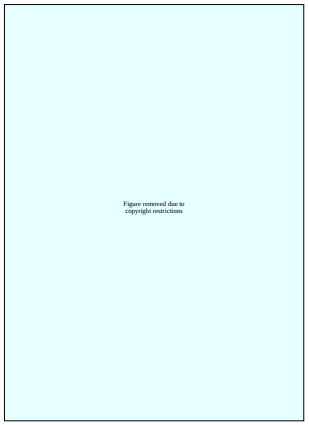

The Ca structure shows an interesting coupling of conductivity and magnetic order. Below ≈ 50 K the material is an antiferromagnetic insulator. In an applied magnetic field, however, the spins can be realigned, also causing a jump in resistivity. Changing the oxygen stoichiometry by Ar or O_2 annealing completely removes the magnetic transition, but does not affect the resistivty, showing that at high fields the magnetic and transport properties are completely decoupled. Oxygen loading can probably rotate the easy magnetization direction in the sample.

JAP 83 (1998) 6992

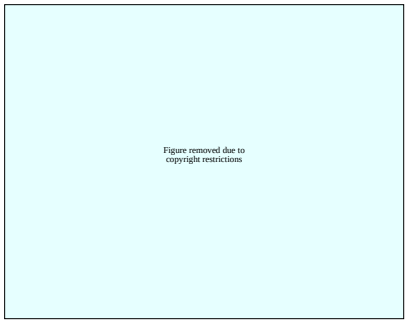

A magnetic phase diagram of $Ca_3Ru_2O_7$. At high magnetic fields the material becomes ferromagnetic metal below 48 K. At higher temperatures it is a paramagnetic metal. There appears to be a multicritical point at 48 K and 4.1 T, marking a narrow region of an unusual antiferromagnetic metal state.

PRL 78 (1997) 1751

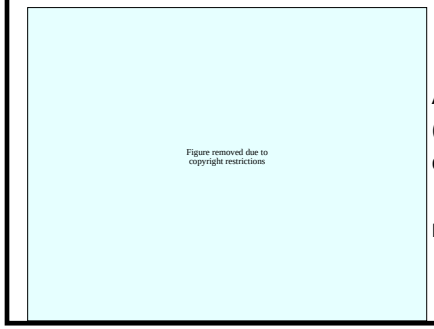

A substitutional phase diagram of the $(Sr_{1-x}Ca_x)_3Ru_2O_7$ system has an even more complex structure.

PRB 56 (1997) 5387

Crystal growth effects

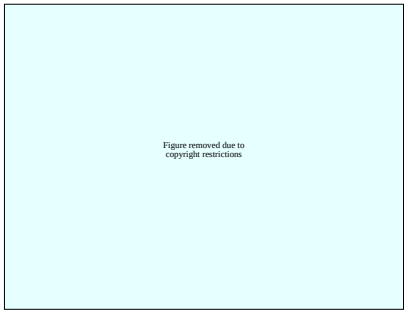

The precise magnetic behavior is very sensitive to the actual crystal growth conditions. Flux grown $Sr_3Ru_2O_7$ crystals become ferromagnetic below 105 K, but floating zone grystals are nonmagnetic with a broad maximum in $\chi(T)$ at around 15 K. $Sr_3Ru_2O_7$ appears to be very close to a ferromagnetic instability and small amounts of impurities or changes in morphology could cause the change. Magnetization curves also depend on the growth method.

Physica B 947-948 (1999) 947

Powder samples are typically synthesized at a temperature of 1300°C. The $Sr_3Ru_2O_7$ phase appears to be somewhat unstable and has to be quenched after oxygen annealing. Slow cooling would result in a partial decomposition into Sr_2RuO_4 and $SrRuO_3$. Even small $SrRuO_3$ impurity can radically change the ferromagnetic signature of a mainly $Sr_3Ru_2O_7$ sample.

References:

Cox92 P. A. Cox, ”Transition Metal Oxides: An Introduction to Their Electronic Structure and Properties”, Clarendon press, Oxford, 1992.